

by true IPR.^{15c} Geminal deuterium substitution of H by D in a second-row main-group element usually gives rise to upfield isotope shifts of -0.01 to -0.03 ppm/D in the ^1H NMR.¹⁶

Furthermore, the value of $^2J_{\text{PH}}$ in the fast-exchange spectrum remains the same for all the isotopomers. This, too, is inconsistent with a nonclassical structure, which should also show isotopic perturbation of the coupling constant because $^2J_{\text{PH}}$ is much larger than $^2J_{\text{PH}_2}$ and so upon deuterium substitution the observed $^2J_{\text{PH}}$ should change significantly due to the isotopic fractionation between classical and nonclassical sites.

Although we were not able to observe decoalescence for the known complexes 4-6,¹⁷ they show similar isotope shifts and minimum T_1 values. We believe that these complexes, too, adopt a classical structure in solution, because of the close analogy of spectroscopic properties for all the complexes 2-6.

The upper limiting value of $T_1(\text{min})$ that we previously suggested^{3b} could be associated with a nonclassical structure is clearly too high. Rather than having a fixed limiting value, it is perhaps better to calculate^{3b,18} values of $T_1(\text{min})$ to be expected on the basis of plausible classical and nonclassical structures for a given compound, and to compare these with the observed numbers. Only if the theoretical numbers are sufficiently different, will the T_1 method be suitable for making a distinction.

Acknowledgment. We thank the National Science Foundation for support, Dr. Peter Demou for assistance, and Dr. J. A. K. Howard for neutron diffraction data.

Note Added in Proof. Cotton and Luck (Cotton, F. A.; Luck, R. J. *Am. Chem. Soc.* 1989, 111, 5757) have suggested that non dipole-dipole (DD) mechanisms are important for $\text{ReH}_2(\text{PPh}_3)_3$ (7). Applying the DD calculation^{3b,11} to their crystallographic H-H distances for 7 leads to a $T_1(\text{min})$ value of 148 ms at 400 MHz, in excellent agreement with their observed $T_1(\text{min})$ value in toluene of 138 ms. We conclude that the DD mechanism is dominant, at least in this case.

Supplementary Material Available: Experimental data including synthetic details for the complexes and their partially deuterated species, details for the calculations and a table of theoretical $T_1(\text{min})$ values (6 pages). Ordering information is given on any current masthead page.

- (16) (a) Bernheim, R. A.; Batiz-Hernandez, H. *J. Chem. Phys.* 1966, 45, 2261. (b) Batiz-Hernandez, H.; Bernheim, R. A. *Prog. NMR Spectrosc.* 1967, 3, 63.
- (17) (a) Chatt, J.; Coffey, R. S. *J. Chem. Soc. A* 1969, 1963. (b) Kelle-Zieher, E. H.; DeWit, D. G.; Caulton, K. G. *J. Am. Chem. Soc.* 1984, 106, 7006.
- (18) (a) This calculation is discussed in the supplementary data and in a forthcoming full paper: Luo, X.-L.; Crabtree, R. H. Manuscript in preparation. (b) The observed $T_1(\text{min})$ values for 2-6 (54-68 ms) are somewhat shorter than the values of 94 (1a) and 107 ms (1b) that we calculate^{3b,18c} at 250 MHz for the ideal classical structures, assuming that they adopt a standard TTP and have a Re-H distance of 1.65 Å and that Re-L_{ax} is inclined 45° to the 3-fold axis. The $T_1(\text{min})$ calculated from the neutron diffraction coordinates^{8a} of 6 gave 77 ms, in reasonable agreement with the observed value of 67 ms. On the other hand, $T_1(\text{min, obs, 250MHz})$ is significantly longer than the theoretical value of 18 ms that we calculate^{3b} for a nonclassical model with $r(\text{H-H})$ of 0.80 Å and $C = 0.8$.^{18b} Only if $r(\text{H-H})$ is as long as 1 Å, does $T_1(\text{min, 250})$ become so long (46 ms) that the T_1 method is no longer able to make a clear-cut structural distinction. (c) In the calculation of a theoretical $T_1(\text{min})$ for a nonclassical hydride, fast rotation of the H₂ ligands seems to be the most reasonable assumption. As shown by Morris et al.,¹⁹ the H₂ protons in such a situation are expected to relax at only 0.25 times the rate that would be found for a nonrotating H₂ ligand. This C factor needs to be considered in arriving at a theoretical relaxation rate only for a nonclassical hydride. This calculation is discussed in detail in the supplementary data.
- (19) Bautista, M. T.; Earl, K. A.; Maltby, P. A.; Morris, R. H. *J. Am. Chem. Soc.* 1988, 110, 7031.

Department of Chemistry
Yale University
New Haven, Connecticut 06511

Xiao-Liang Luo
Robert H. Crabtree*

Received April 25, 1989

A High-Potential Mononuclear Manganese(IV) Complex. Synthesis, Structure, and Properties, Including EPR Spectroscopy and Electrochemistry, of $[\text{Mn}(\text{HB}(3,5\text{-Me}_2\text{pz})_3)_2](\text{ClO}_4)_2$ (pz = Pyrazolyl)

A resurgence of interest in higher valent manganese chemistry in recent years stems from the realization of its importance in biological processes such as photosynthetic water oxidation,¹ superoxide dismutation,² and peroxide disproportionation.³ The S₂ state of the oxygen-evolving complex of photosystem II displays a multiline EPR⁴ signal centered at $g = 2.0$ as well as a prominent $g = 4.1$ signal, both of which are associated with the manganese center.⁵ Although it is generally agreed that the multiline signal originates from a multinuclear manganese center, the source of the $g = 4.1$ signal is not well understood. Recently, Hansson, Aasa, and Vänngård (HAV)⁶ postulated that the $g = 4.1$ signal arises from a mononuclear Mn(IV) center that is in redox equilibrium with a separate polynuclear site. If one assumes that (i) water oxidation occurs at the multiline site and (ii) there is a relatively small separation between the Mn^{IV}/Mn^{III} reduction potential of the putative mononuclear $g = 4.1$ site and that of the multiline site, then the $g = 4.1$ site is required to have a rather high reduction potential, perhaps in the vicinity of ~ 1 V vs NHE. While several Mn(IV) species have been characterized,⁷ very few have reduction potentials of ≥ 1.0 V. Here we report the synthesis, structure, and properties of a novel Mn(IV) complex that is noteworthy in the

- (1) (a) Brudvig, G. W. In *Metal Clusters in Proteins*; Que, L., Jr., Ed.; ACS Symposium Series 372; American Chemical Society: Washington, DC, 1988; pp 221-237. (b) Pecoraro, V. L. *Photochem. Photobiol.* 1988, 48, 249-264. (c) Babcock, G. T. In *New Comprehensive Biochemistry: Photosynthesis*; Ames, J., Ed.; Elsevier: Amsterdam, 1987; pp 125-158. (d) Dismukes, G. *Photochem. Photobiol.* 1986, 43, 99-115. (e) Govindjee; Kambara, T.; Coleman, W. *Photochem. Photobiol.* 1985, 42, 187-210.
- (2) Michelson, J. M.; McCord, J. M.; Fridovich, I., Eds.; *Superoxide and Superoxide Dismutases*; Academic: New York, 1977.
- (3) (a) Beyer, W. F.; Fridovich, I. *Biochemistry* 1985, 24, 6460-6467. (b) Kono, Y.; Fridovich, I. *J. Biol. Chem.* 1983, 258, 6015-6019. (c) Fronko, R. M.; Penner-Hahn, J. E. *J. Am. Chem. Soc.* 1988, 110, 7554-7555.
- (4) Abbreviations used: EPR, electron paramagnetic resonance; cp, cyclopentadienyl; SCE, saturated calomel electrode; SSCE, sodium saturated calomel electrode; pz, pyrazolyl; H₂saladh_p, 1,3-dihydroxy-2-methyl-2-(salicylideneamino)propane; H₂sal, salicylic acid; dtbc, 3,5-di-*tert*-butylcatecholato; py, pyridine; TPP, 5,10,15,20-tetraphenylporphyrinato; bpy, 2,2'-bipyridine; phen, 1,10-phenanthroline; tren, 2,2',2''-triaminotriethylamine; terpyO, 2,2':6',2''-terpyridine 1,1',1''-trioxide; H₂Salah_p, 1-hydroxy-3-(salicylideneamino)propane; H₂hps, N-(2-hydroxyphenyl)salicylamide; PS II, photosystem II.
- (5) (a) Cole, J.; Yachandra, V. K.; Guiles, R. D.; McDermott, A. E.; Britt, R. D.; Dexheimer, S. L.; Sauer, K.; Klein, M. P. *Biochim. Biophys. Acta* 1987, 890, 395-398. (b) Zimmermann, J.-L.; Rutherford, A. W. *Biochemistry* 1986, 25, 4609-4615.
- (6) Hansson, Ö.; Aasa, R.; Vänngård, T. *Biophys. J.* 1987, 51, 825-832.
- (7) Representative examples: (a) Kessissoglou, D. P.; Li, X.; Butler, W. M.; Pecoraro, V. L. *Inorg. Chem.* 1987, 26, 2487-2492. (b) Kessissoglou, D. P.; Butler, W. M.; Pecoraro, V. L. *J. Chem. Soc., Chem. Commun.* 1986, 1253-1255. (c) Pavacic, P. S.; Huffman, J. C.; Christou, G. *J. Chem. Soc., Chem. Commun.* 1986, 43-44. (d) Pal, S.; Ghosh, P.; Chakravorty, A. *Inorg. Chem.* 1985, 24, 3704-3706. (e) Fujiwara, M.; Matsushita, T.; Shono, T. *Polyhedron* 1985, 4, 1895-1900. (f) Matsushita, T.; Hirata, Y.; Shono, T. *Bull. Chem. Soc. Jpn.* 1982, 55, 108-112. (g) Camenzind, M. J.; Hollander, F. J.; Hill, C. L. *Inorg. Chem.* 1983, 22, 3776-3784. (h) Camenzind, M. J.; Hollander, F. J.; Hill, C. L. *Inorg. Chem.* 1982, 21, 4301-4308. (i) Brown, K. L.; Golding, R. M.; Healy, P. C.; Jessop, K. J.; Tennant, W. C. *Aust. J. Chem.* 1974, 27, 2075-2081. (j) Hendrickson, A. R.; Martin, R. L.; Rohde, N. M. *Inorg. Chem.* 1974, 13, 1933-1939. (k) Chin, D.-H.; Sawyer, D. T.; Schaefer, W. P.; Simmons, C. J. *Inorg. Chem.* 1983, 22, 752-758. (l) Richens, D. T.; Sawyer, D. T. *J. Am. Chem. Soc.* 1979, 101, 3681-3683. (m) Hartman, J. R.; Foxman, B. M.; Cooper, S. R. *Inorg. Chem.* 1984, 23, 1381-1387. (n) Lynch, M. W.; Hendrickson, D. N.; Fitzgerald, B. J.; Pierpont, C. G. *J. Am. Chem. Soc.* 1984, 106, 2041-2049. (o) Koikawa, M.; Okawa, H.; Kida, S. *J. Chem. Soc., Dalton Trans.* 1988, 641-645. (p) Howard, C. G.; Girolami, G. S.; Wilkinson, G.; Thornton-Pett, M.; Hursthouse, M. B. *J. Chem. Soc., Chem. Commun.* 1983, 1163-1164. (q) Andersen, R. A.; Carmona-Guzman, E.; Gibson, J. F.; Wilkinson, G. *J. Chem. Soc., Dalton Trans.* 1976, 2204-2211. (r) Bukovec, P.; Hoppe, R. *J. Fluorine Chem.* 1983, 23, 579-587. (s) Moews, P. C., Jr. *Inorg. Chem.* 1966, 5, 5-8.

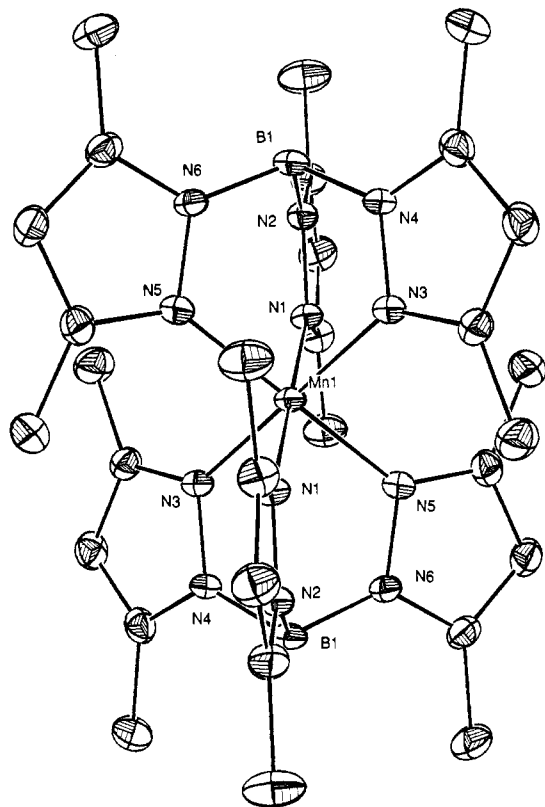


Figure 1. Structure of $[\text{Mn}(\text{HB}(3,5\text{-Me}_2\text{pz})_3)_2]^{2+}$ (cation of **1**) showing the 50% probability thermal ellipsoids and atom-labeling scheme. Hydrogen atoms are omitted for clarity. Selected interatomic distances (\AA) and angles (deg) are as follows: $\text{Mn}(1)\text{-N}(1) = 1.976$ (3), $\text{Mn}(1)\text{-N}(3) = 1.967$ (3), $\text{Mn}(1)\text{-N}(5) = 1.971$ (2); $\text{N}(1)\text{-Mn}(1)\text{-N}(3) = 89.8$ (1), $\text{N}(1)\text{-Mn}(1)\text{-N}(5) = 90.2$ (1), $\text{N}(1)\text{-Mn}(1)\text{-N}(5) = 90.7$ (1), $\text{N}(1)\text{-Mn}(1)\text{-N}(5') = 89.3$ (1), $\text{N}(3)\text{-Mn}(1)\text{-N}(5) = 90.3$ (1), $\text{N}(3)\text{-Mn}(1)\text{-N}(5') = 89.7$ (1). Bond distances and angles for the crystallographically independent cation are as follows: $\text{Mn}(2)\text{-N}(7) = 1.972$ (2), $\text{Mn}(2)\text{-N}(9) = 1.966$ (3), $\text{Mn}(2)\text{-N}(11) = 1.982$ (3); $\text{N}(7)\text{-Mn}(2)\text{-N}(9) = 90.0$ (1), $\text{N}(7)\text{-Mn}(2)\text{-N}(9') = 90.0$ (1), $\text{N}(7)\text{-Mn}(2)\text{-N}(11) = 91.0$ (1), $\text{N}(7)\text{-Mn}(2)\text{-N}(11') = 89.0$ (1), $\text{N}(9)\text{-Mn}(2)\text{-N}(11) = 90.3$ (1), $\text{N}(9)\text{-Mn}(2)\text{-N}(11') = 89.8$ (1).

context of the HAV model and that to our knowledge possesses the highest IV/III reduction potential among isolated Mn^{IV} complexes (1.35 V vs SSCE).

Bis(hydrotri-*i*-pyrazolylborate) complexes of divalent and, to a lesser extent, trivalent first-row transition elements are well-known.⁸ The synthesis of $[\text{Mn}(\text{HB}(3,5\text{-Me}_2\text{pz})_3)_2](\text{ClO}_4)_2$ (**1**) was initiated by adding 0.673 g (2.00 mmol) of $\text{KHB}(3,5\text{-Me}_2\text{pz})_3$ to a solution of 0.887 g (2.45 mmol) of $\text{Mn}(\text{ClO}_4)_2 \cdot 6\text{H}_2\text{O}$ in 50 mL of acetone/ H_2O (60/40, v/v). Addition of 0.316 g (1.97 mmol) of NaMnO_4 resulted in precipitation of a brown solid. Treatment of this solid with 60% aqueous HClO_4 , followed by extraction with 50 mL of CH_3CN , gave a deep blue solution. Concentration by evaporation, followed by filtration, afforded 0.611 g (72.0% yield) of deep blue crystals of **1** suitable for elemental analysis and X-ray diffraction studies.⁹ Attempts to prepare an analogous $\text{Mn}(\text{IV})$ species with HBpz_3^- were successful; however, the material isolated contained $[\text{Mn}(\text{H}_2\text{O})_6]^{2+}$ as well as the Mn^{IV} cation, as determined by X-ray crystallography.¹⁰

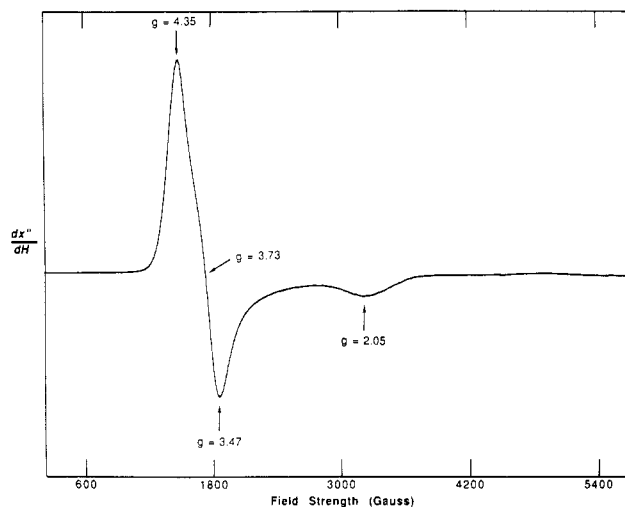


Figure 2. X-Band ($\nu = 9.32$ GHz) EPR spectrum of **1** in CH_3CN at 77 K with the following instrument settings: microwave power, 12.6 mW; field modulation amplitude, 36 G; modulation frequency, 100 kHz; receiver gain, 6.3×10^2 .

The synthetic route used to prepare this complex, $[\text{Mn}(\text{HBpz}_3)_2][\text{Mn}(\text{H}_2\text{O})_6](\text{ClO}_4)_4$ (**2**), was similar to that used for **1**.

The crystal structure of **1** consists of two independent centrosymmetric $[\text{Mn}(\text{HB}(3,5\text{-Me}_2\text{pz})_3)_2]^{2+}$ complexes and well-separated perchlorate anions on general positions. Compound **1** is one of the few structurally characterized M^{4+} species in an N_6 coordination environment.¹¹ A representation of one of the cations is shown in Figure 1. The manganese coordination environment is nearly octahedral with $\text{Mn}\text{-N}$ bond distances in the range 1.966 (3)–1.982 (3) \AA and cis $\text{N}\text{-Mn}\text{-N}$ angles between 89.0 (1) and 90.7 (1) $^\circ$ for both of the cations in **1**. Trans $\text{N}\text{-Mn}\text{-N}$ angles are required to be 180° , owing to the crystallographic inversion center. Thus, the cation closely approaches D_{3d} point symmetry. Average $\text{Mn}\text{-N}$ bond distances in **1** (1.972 \AA) and **2** (1.955 \AA)¹¹ are somewhat shorter than the average $\text{Mn}^{\text{IV}}\text{-N}$ separations in $[\text{Mn}(\text{saladhp})_2]$ (2.005 \AA),^{7a} $[\text{Mn}(\text{sal})_2(\text{bpy})]$ (2.047 \AA),^{7c} $[\text{Mn}(\text{dtbc})_2(\text{py})_2]$ (2.018 \AA),⁷ⁿ $[\text{MnTPP}(\text{OMe})_2]$ (2.012 \AA),^{7h} $[\text{Mn}_2\text{O}_2(\text{bpy})_4]^{3+}$ (2.049 \AA),¹² $[\text{Mn}_2\text{O}_2(\text{phen})_4]^{4+}$ (2.043 \AA),¹³ and $[\text{Mn}_2\text{O}_2(\text{tren})_2]^{3+}$ (2.073 \AA).¹⁴

The electronic absorption spectra of **1** and **2** are dominated by intense charge-transfer transitions at 599 nm ($\epsilon = 12\,000$ $\text{M}^{-1}\text{cm}^{-1}$) and 545 nm ($\epsilon = 12\,000$ $\text{M}^{-1}\text{cm}^{-1}$), respectively. Electron-donating properties of the methyl groups in **1** may account for the lower energy absorption in this case. Magnetic susceptibility data at room temperature in the solid state (3.81 μ_B) confirm a d^3 electronic configuration.

The EPR behavior of **1** was of particular interest, owing to the possibility that the $g = 4.1$ signal in photosystem II arises from

(8) Trofimenko, S. *Prog. Inorg. Chem.* **1986**, *34*, 115–210.

(9) Anal. Calcd for $\text{C}_{30}\text{H}_{44}\text{B}_2\text{Cl}_2\text{MnN}_{12}\text{O}_8$: C, 42.48; H, 5.23; Cl, 8.36; Mn, 6.48; N, 19.81. Found: C, 42.79; H, 5.39; Cl, 8.53; Mn, 6.08; N, 20.18. X-ray analysis of **1**: This compound crystallizes in the triclinic system, space group $P\bar{1}$, with $a = 10.694$ (2) \AA , $b = 11.535$ (2) \AA , $c = 16.231$ (5) \AA , $\alpha = 78.66$ (2) $^\circ$, $\beta = 81.45$ (2) $^\circ$, $\gamma = 73.16$ (2) $^\circ$, $V = 1870$ (1) \AA^3 , $\rho_{\text{calcd}} = 1.51$ g cm^{-3} , and $Z = 2$. Data collection at 158 K out to 46° in 2θ provided 4198 reflections with $I > 3\sigma(I)$. The structure was solved by Patterson and direct methods (SHELXS86) and refined by using 499 parameters to final R (R_w) values of 3.84% (5.38%).

- (10) X-ray analysis: Compound **2** crystallizes in the triclinic system, space group $P\bar{1}$, with $a = 9.328$ (2) \AA , $b = 9.425$ (3) \AA , $c = 13.227$ (3) \AA , $\alpha = 105.20$ (2) $^\circ$, $\beta = 86.63$ (2) $^\circ$, $\gamma = 119.21$ (2) $^\circ$, $V = 976.3$ (4) \AA^3 , $\rho_{\text{calcd}} = 1.77$ g cm^{-3} , and $Z = 1$. Data collection at 130 K out to $2\theta = 55^\circ$ afforded 3949 reflections with $I > 3\sigma(I)$. The structure was solved by a combination of Patterson and direct methods (SHELXS86) and refined using 304 parameters to final R (R_w) values of 3.55% (4.28%). Both Mn^{II} and Mn^{IV} complexes are on inversion centers. Interatomic distances (\AA) and angles (deg) are as follows: $\text{Mn}(1)\text{-N}(1) = 1.960$ (2), $\text{Mn}(1)\text{-N}(3) = 1.957$ (2), $\text{Mn}(1)\text{-N}(5) = 1.948$ (2), $\text{Mn}(2)\text{-O}(10) = 2.174$ (2), $\text{Mn}(2)\text{-O}(11) = 2.168$ (2), $\text{Mn}(2)\text{-O}(12) = 2.189$ (2); $\text{N}(1)\text{-Mn}(1)\text{-N}(3) = 88.9$ (1), $\text{N}(1)\text{-Mn}(1)\text{-N}(5) = 88.7$ (1), $\text{N}(3)\text{-Mn}(1)\text{-N}(5) = 88.4$ (1), $\text{N}(1)\text{-Mn}(1)\text{-N}(3') = 91.1$ (1), $\text{N}(1)\text{-Mn}(1)\text{-N}(5') = 91.3$ (1), $\text{N}(3)\text{-Mn}(1)\text{-N}(5') = 91.6$ (1).
- (11) (a) Mikami, M.; Konno, M.; Saito, Y. *Acta Crystallogr.* **1979**, *B35*, 3096–3098. (b) Schollhorn, H.; Beyerle-Pfnur, R.; Thewalt, U.; Lippert, B. *J. Am. Chem. Soc.* **1986**, *108*, 3680–3688.
- (12) Plaskin, P. M.; Stouffer, R. C.; Mathew, M.; Palenik, G. *J. Am. Chem. Soc.* **1972**, *94*, 2121–2122.
- (13) Stebler, M.; Ludi, A.; Burgi, H.-B. *Inorg. Chem.* **1986**, *25*, 4743–4750.
- (14) Hagen, K. S.; Armstrong, W. H.; Hope, H. *Inorg. Chem.* **1988**, *27*, 967–969.

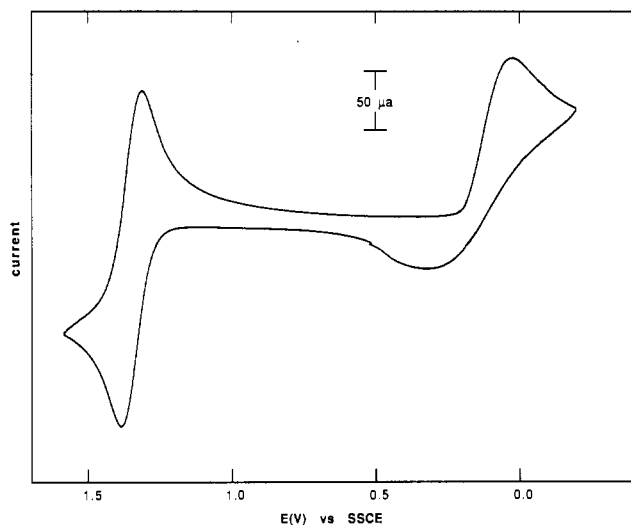


Figure 3. Cyclic voltammogram of **1** in CH_3CN with 0.100 M Et_4NClO_4 as supporting electrolyte, a Pt working electrode, a Pt-wire counter electrode, an SSCE reference electrode, and a scan speed of 50 mV/s.

a mononuclear Mn(IV) center. The EPR spectrum of a crude sample of **1** resembled that reported recently for a tris(thiohydroxamato)manganese(IV) complex,^{7d} with signals in the $g = 4$ and $g = 2$ regions. However, after purification most of the absorption in the $g = 2$ region was removed. The resulting spectrum, shown in Figure 2, is similar to that reported for $[\text{MnTPP}(\text{NCO})_2]^{7g}$ except that hyperfine splitting in the $g = 2$ region was observed for the porphyrin complex. In contrast to the expectation that nearly octahedral coordination around Mn in **1** may give rise to a small axial zero-field splitting parameter (D), the data are consistent instead with a relatively large D value ($2D \gg h\nu \approx 0.31 \text{ cm}^{-1}$ at X-band frequencies).^{15,16} The asymmetric appearance of the low-field signal and the fact that the crossing point of the same signal is at $g < 4$ (3.73) reveal a noticeable rhombic distortion. Despite the greater rhombicity in **1**, there is a distinct resemblance between its EPR spectrum in the low-field region and that of the $g = 4.1$ signal in PS II. This result supports the HAV model to the extent that it provides an example of a Mn(IV) species in a non-heme environment with a nearly axial EPR spectrum devoid of detectable ^{55}Mn nuclear hyperfine coupling in the $g = 4$ region.

The cyclic voltammogram of **1**, shown in Figure 3, reveals a quasi-reversible wave corresponding to the $\text{Mn}^{\text{IV}}/\text{Mn}^{\text{III}}$ couple (1.35 V vs SSCE) and an irreversible III/II couple with $E_{\text{p,c}} = 0.02 \text{ V}$. To our knowledge compound **1** has the highest $\text{Mn}^{\text{IV}}/\text{Mn}^{\text{III}}$ reduction potential among mononuclear complexes which have been isolated in their Mn^{IV} form. On the other hand, a higher IV/III couple has been reported for a complex isolated in the Mn^{II} form, $[\text{Mn}(\text{terpyO}_3)]^{2+}$ (1.77 V vs SCE).¹⁷ Compound **1** may find use as a high-potential one-electron outer-sphere oxidizing agent. Complexes commonly used for this purpose include $\text{Fe}(\text{cp})_2^+$ ($E_{1/2} = 0.307 \text{ V vs SCE}$)¹⁸ and Ce^{4+} (1.20 V vs SCE).¹⁹ Whereas the pyrazolylborate ligands in **1** destabilize Mn^{IV} with respect to Mn(III), alkoxide or deprotonated amide donors greatly stabilize the Mn(IV) level, as is illustrated by the low reduction potentials for $[\text{Mn}(\text{salahp})_2]$ ($E_{\text{p,c}} = -0.32 \text{ V vs Ag/AgCl}$)^{7a} and $[\text{Mn}(\text{hps})_2]^{2+}$ ($E_{1/2} = -0.89 \text{ V vs SCE}$).^{7o}

In conclusion, a novel Mn(IV) species with a nearly octahedral N_6 coordination environment has been isolated and characterized by X-ray crystallography, magnetic susceptibility, electrochemical, and spectroscopic measurements. Magnetic susceptibility and EPR data support the Mn(IV) formulation. In addition to contributing

to the understanding of Mn(IV) species, **1** should find use as a high-potential oxidant. Finally, $[\text{Mn}(\text{HB}(3,5\text{-Me}_2\text{pz})_3)_2]^{2+}$ may serve as a model for the Mn species that gives rise to the $g = 4.1$ signal in PS II.²⁰

Acknowledgment. This work was supported by Grant No. GM382751-01 from the National Institute of General Medical Sciences. We thank Drs. Frederick J. Hollander and Marilyn M. Olmstead for assistance with the X-ray structure determinations. We are grateful to Professor K. Sauer and Dr. M. Klein, who kindly provided a preprint of ref 21.

Registry No. 1, 122189-07-5; 2, 122174-20-3.

Supplementary Material Available: For both **1** and **2**, fully labeled ORTEP drawings and tables of positional and isotropic thermal parameters, anisotropic thermal parameters, interatomic distances, and interatomic angles (25 pages). Ordering information is given on any current mast-head page.

(20) A reviewer suggested that since it is generally thought that the environment around manganese in PS II consists of exclusively oxygen donors, compound **1** may have little relevance. However, this notion is usually based on spin-echo EPR results,²¹ which apply *only* to the multiline site. No conclusions pertaining to the identity of ligands at the $g = 4.1$ center can be drawn from these observations. A recent report by Inoue et al.²² suggests that histidine may be coordinated to manganese in PS II.

(21) Britt, R. D.; DeRose, V. J.; Chan, M. K.; Armstrong, W. H.; Sauer, K.; Klein, M. P. Submitted for publication.

(22) Tamura, N.; Ikeuchi, M.; Inoue, Y. *Biochim. Biophys. Acta* **1989**, *973*, 281-289.

Department of Chemistry
University of California
Berkeley, California 94720

Michael K. Chan
William H. Armstrong*

Received September 29, 1988

Aerobic and Anaerobic Photooxidation of *p*-Xylene in the Presence of Phosphotungstic Acid and Its Tetrabutylammonium Salt

Iso- and heteropolyoxoanions (POA) have been described as soluble analogues of transition-metal oxides, amenable to chemical tailoring and detailed characterization at a molecular level.¹⁻⁴ Recent interest in their chemistry has been fostered by their ability to mimic the interactions between organic substrates and catalytic oxide surfaces⁵⁻⁸ and to promote the thermal or photochemical selective oxidation of these substrates.⁹⁻¹¹

- (15) Pedersen, E.; Toftlund, H. *Inorg. Chem.* **1974**, *13*, 1603-1612.
(16) Hempel, J. C.; Morgan, L. O.; Lewis, W. B. *Inorg. Chem.* **1970**, *9*, 2064-2072.
(17) Morrison, M. M.; Sawyer, D. T. *Inorg. Chem.* **1978**, *17*, 338-339.
(18) Bard, A. J.; Faulkner, L. R. *Electrochemical Methods*; Wiley: New York, 1980; p 701.
(19) Reference 18, p 699.

- (1) Pope, M. T. *Heteropoly and Isopoly Oxometalates*; Springer-Verlag: Berlin, 1983.
(2) Pope, M. T. *Mixed-Valence Compounds*; Brown, D. B., Ed.; NATO ASI Series C58; D. Reidel Publ. Co.: Dordrecht, The Netherlands, 1980; p 365.
(3) Krebs, B. *Transition Metal Chemistry*; Mueller, A., Diemann, E., Eds.; Verlag Chemie: Weinheim, FRG, 1981; p 79.
(4) Day, V. W.; Klemperer, W. G. *Science* **1985**, *228*, 533.
(5) Prosser-McCartha, C. M.; Kadkhodayan, M.; Williamson, M. M.; Bouchard, D. A.; Hill, C. L. *J. Chem. Soc., Chem. Commun.* **1986**, 1747.
(6) Day, V. W.; Thompson, M. R.; Day, C. S.; Klemperer, W. G.; Liu, R. S. *J. Am. Chem. Soc.* **1980**, *102*, 5971.
(7) McCarron, E. M., III; Harlow, R. L. *J. Am. Chem. Soc.* **1983**, *105*, 6179.
(8) McCarron, E. M., III; Staley, R. H.; Sleight, A. W. *Inorg. Chem.* **1984**, *23*, 1043.
(9) Hill, C. L.; Bouchard, D. A. *J. Am. Chem. Soc.* **1985**, *107*, 5148.
(10) Fox, M. A.; Cardona, R.; Gaillard, E. *J. Am. Chem. Soc.* **1987**, *109*, 6347.
(11) Papacostantinou, E. *J. Chem. Soc., Chem. Commun.* **1982**, 12.